Article

Asymmetric Hydrogenation of #-Boryl Enamides Enabled by Nonbonding Interactions

Dongyang Fan, Jian Zhang, Yanhua Hu, Zhenfeng Zhang, Ilya D. Gridnev, and Wanbin Zhang

ACS Catal., **Just Accepted Manuscript** • DOI: 10.1021/acscatal.9b04543 • Publication Date (Web): 10 Feb 2020

Asymmetric Hydrogenation of α-Boryl Enamides Enabled by Nonbonding Interactions

Dongyang Fan,[†] Jian Zhang,[†] Yanhua Hu,[‡] Zhenfeng Zhang,[,†] Ilya D. Gridnev,[*,§] and Wanbin Zhang[*,†,‡]*

[†]Shanghai Key Laboratory for Molecular Engineering of Chiral Drugs, School of Pharmacy, Shanghai Jiao Tong University, 800 Dongchuan Road, Shanghai 200240, P. R. China

[‡]School of Chemistry and Chemical Engineering, Shanghai Jiao Tong University, 800 Dongchuan Road, Shanghai 200240, P. R. China

[§]Department of Chemistry, Graduate School of Science, Tohoku University, Aramaki 3-6, Aoba-ku, Sendai 980-8578, Japan

ABSTRACT: The asymmetric hydrogenation of α-boryl enamides has been developed using a bisphosphine-rhodium catalyst. The chelate coordination of the amido group to rhodium and the nonbonding interactions between the substrate and ligand play important roles to afford chiral α-amidoboronic esters with quantitative conversions, high chemoselectivity, and excellent enantioselectivity (92-99% ee). Computation of the catalytic cycle revealed selectivity both in the hydrogen activation and migratory insertion steps equally contributing to the high enantioselectivity. In both cases the nonbonding interactions provided by the Bpin group contributed significantly to the stabilization of the transition states in the lower energy pathway.

KEYWORDS: asymmetric hydrogenation • rhodium • α-boryl enamides • α-aminoboronic acid • nonbonding interaction

■ INTRODUCTION

Organoboron compounds are popular in the chemical and pharmaceutical fields owing to their unique physical, chemical, and bioactive properties.[1] The Nobel Prize in chemistry has been awarded to the development of boron-related reagents and reactions three times (1976, 1979, 2010). Recently, chiral organoboron compounds have attracted much attention due to their broad utilization in drug discovery and synthetic applications.[2] Among them, chiral α-aminoboronic acids, as mimics of chiral amino acids, are one of the most significant fragments in many important pharmaceuticals, such as Bortezomib (marketed as Velcade®) and Ixazomib citrate (marketed as Ninlaro®) (Figure 1).[3]

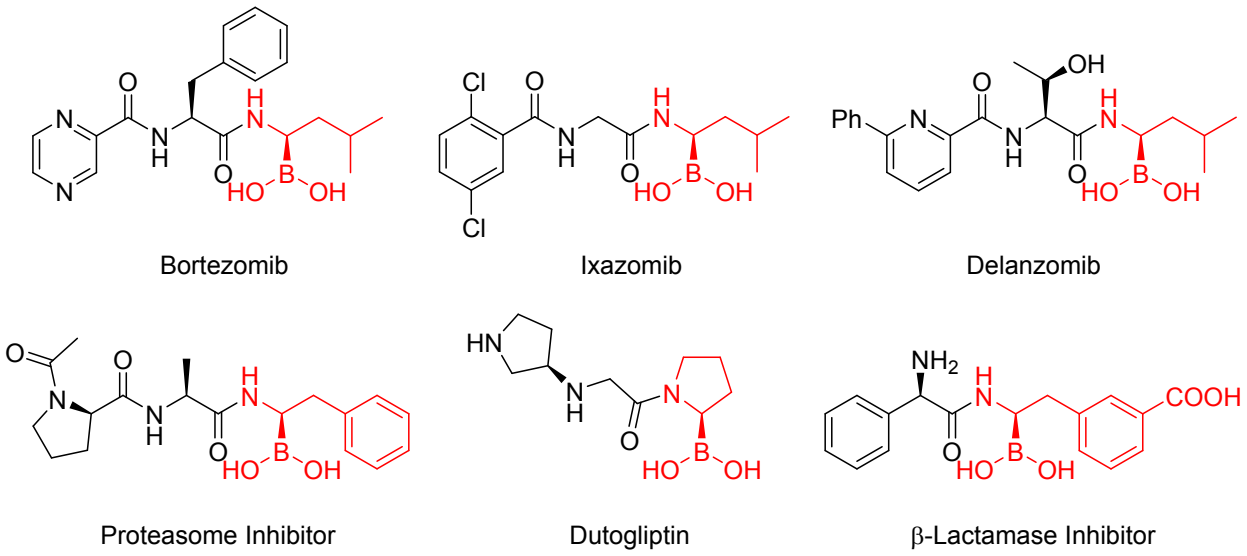

Figure 1. Pharmaceutically important compounds bearing chiral α-aminoboronic acid fragments.

The importance of chiral α-aminoboronic acid derivatives has promoted the development of their asymmetric synthesis. The most common route is a diastereoselective method that utilizes chiral auxiliaries to synthesize chiral α-aminoboronic esters.[4] A lithiation-borylation protocol

has also been developed mediated by chiral sparteine or starting from chiral amines.[5] However, such methods are unsatisfactory since they require stoichiometric amounts of chiral reagents. In contrast, asymmetric catalytic routes for the synthesis of chiral α-aminoboronic acid derivatives are supposed to be more economic but are not as widely reported. The asymmetric borylation of imines or enamines is one of the most feasible approaches to furnish chiral α-aminoboronic esters (Scheme 1a and 1b).[6] Another method to afford the target compounds is the asymmetric amination of alkenylboronates (Scheme 1c).[7] However, high catalyst loadings and a large dosage of boron-, silicon-, nitrogen-containing reagents reduces the practicality of the process and increases problems in scale-up. Therefore, it is highly desirable to develop a more efficient and green method for the construction of chiral α-aminoboronic acid derivatives.

Transition-metal-catalyzed asymmetric hydrogenation is considered to be one of the most efficient and green routes for the synthesis of chiral compounds.[8] It has shown extremely high performance in the synthesis of chiral α-amino acid derivatives via asymmetric hydrogenation of α-acyl enamides (Scheme 1d).[9] However, the enantioselective synthesis of their analogues, chiral α-aminoboronic acid derivatives, has not yet been realized via the asymmetric hydrogenation of α-boryl enamides, even though this method seems to be a natural and feasible solution. The reason lies in the challenge with regards to high chemoselectivity between hydrogenation and hydrodeboronation, as well as high stereoselectivity.[10] It was envisaged that the presence of a chelating amido group at the α-position to the boryl group would be advantageous for chemoselectivity. Additionally, one could expect that the Bpin group is capable of several kinds of weak nonbonding interactions enabling it to act as a directing group to provide high stereoselectivity.[11] Along with our continuing research on asymmetric hydrogenation,[11,12] herein we report the chemo- and enantioselective synthesis of chiral α-

aminoboronic acid derivatives via asymmetric hydrogenation using α-boryl enamides as the substrates and BenzP*-Rh[13] as the catalyst (Scheme 1e).

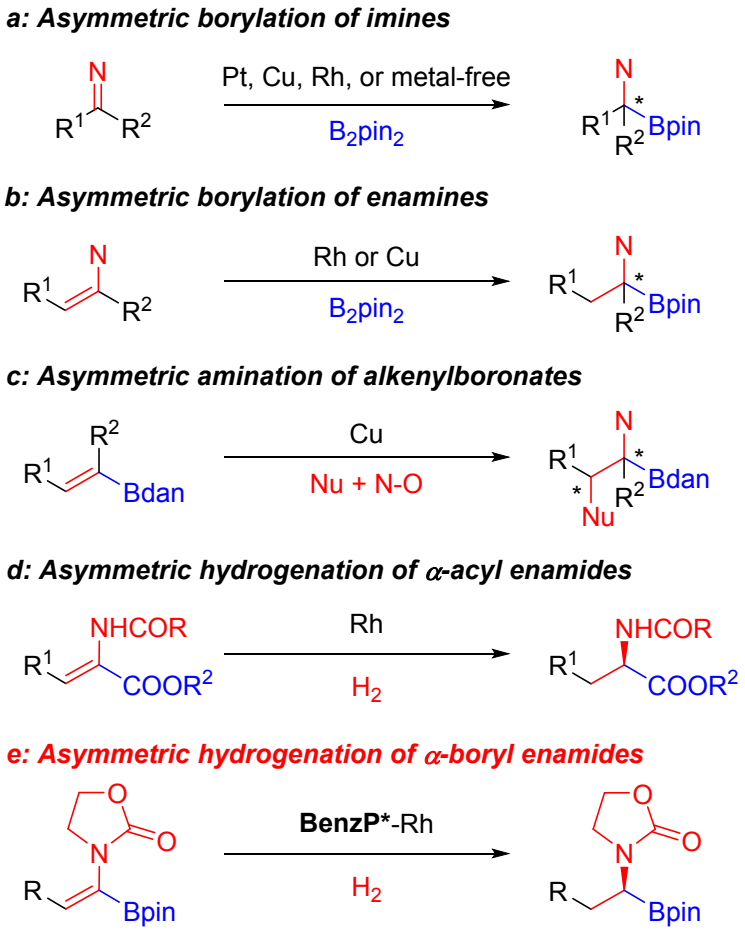

Scheme 1. Catalytic Enantioselective Synthesis of Chiral α-Aminoboronic Acid Derivatives

■ RESULTS AND DISCUSSION

Looking for appropriate substrates, we first considered **1a-NH** as the one having a simple structure. Unfortunately, our attempts to prepare **1a-NH** were unsuccessful. This initiated the search for alternative precursors and resulted in finding a substrate **1a** with a five-membered oxazolidinonyl group, which can be readily synthesized according to the procedure reported by Zhu et al.[14] Actually, **1a** may be a better substrate than **1a-NH**, since the optimized structure of **1a** shows a larger BC-NC twist angle of 37.5°, a larger N-C-O angle of 127.1°, and a longer

O···B bond length of 2.85 Å compared to those computed for **1a-NH** (Figure 2), which may be advantageous for the coordination of the C=O and C=C bonds with the Rh atom. Indeed, substrate **1a** underwent smooth hydrogenation catalyzed by a BenzP*-Rh complex, affording the desired product in 99% conversion and with 95% ee (Table 1, entry 1).

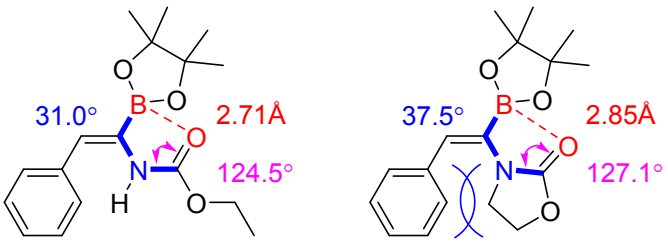

1a-NH **1a**

Figure 2. Representative substrates.

Table 1 shows the chiral diphosphine ligands that were tested in the Rh-catalyzed hydrogenation of **1a** carried out in dichloromethane (DCM) under 30 atm hydrogen pressure (Table 1). Using the centrally chiral ligand NorPhos, the desired product was obtained with poor chemoselectivity and moderate enantioselectivity. The hydrogenation in this case was characterized by low conversion together with formation of some amount of the deboronated by-products **2a'** and **2a''**. The axially chiral ligand BINAP exhibited moderate conversion, excellent chemoselectivity, and poor enantioselectivity. The conversions and chemoselectivities were dramatically improved by using the planarly chiral ligands PhanePhos and JosiPhos, although the enantioselectivities were still poor. The ligand Me-FcPhos, bearing electron-rich phosphine groups on a ferrocene skeleton, gave the desired product in quantitative conversion but with poor enantioselectivity. Another typical electron-rich ligand Me-DuPhos, possessing the same phosphine groups as Me-FcPhos, afforded a positive enantioselectivity but unsatisfactory chemoselectivity. Both excellent chemoselectivity and enantioselectivity were only obtained by

using the P-stereogenic ligand BenzP* possessing electron-rich *tert*-butylmethylphosphino groups. The same excellent enantioselectivity of 95% was observed with another P-stereogenic ligand QuinoxP* that demonstrates the importance of the *t*-Bu groups on the ligand for high enantioselectivity in this reaction. Further optimization was focused on the screening of solvents using the BenzP*-Rh catalyst. Another halogenated solvent, dichloroethane (DCE), gave a higher enantioselectivity of 98% ee but lower conversion (entry 2 vs 1). Reaction in less polar solvents such as tetrahydrofuran (THF), dimethyl ethyl diether (DME), and toluene also showed high chemo- and enantioselectivity with incomplete conversion (entries 3-5). A better result was obtained using ethyl acetate (EtOAc) as the solvent (entry 6). The desired product was obtained without any loss of conversion and ee when the hydrogen pressure was reduced from 30 atm to 5 atm (entries 7-8). Further reduction of the hydrogen pressure to 1 atm gave incomplete conversion with retention of enantioselectivity (entry 9). The hydrogenation of **1a** was also completed using 1 mol % catalyst, affording the desired product **2a** in 99% conversion and 96% ee (entry 10).

With the optimized reaction conditions in hand, we set out to study the substrate scope of α-boryl enamides in this hydrogenation (Scheme 2). It was found that the substituted positions and electronic properties of the substituents had a great impact on reactivities as well as enantioselectivities. Substrates bearing small substituents at the *para*-position showed higher activity (**2f**, **2n**, **2p**, **2q**, and **2t**), while other substrates required a 2 mol % catalyst loading to complete the hydrogenation (**2b-d**, **2g-k**, **2o**, **2r**, and **2s**), and the last three substrates needed a 4 mol % catalyst loading for complete hydrogenation (**2e**, **2l**, and **2m**). Generally, the electron-withdrawing substituted substrates exhibited slightly better enantioselectivities compared with the electron-donating substituted substrates. When a halogen was substituted on the phenyl ring,

Table 1. Condition Optimization

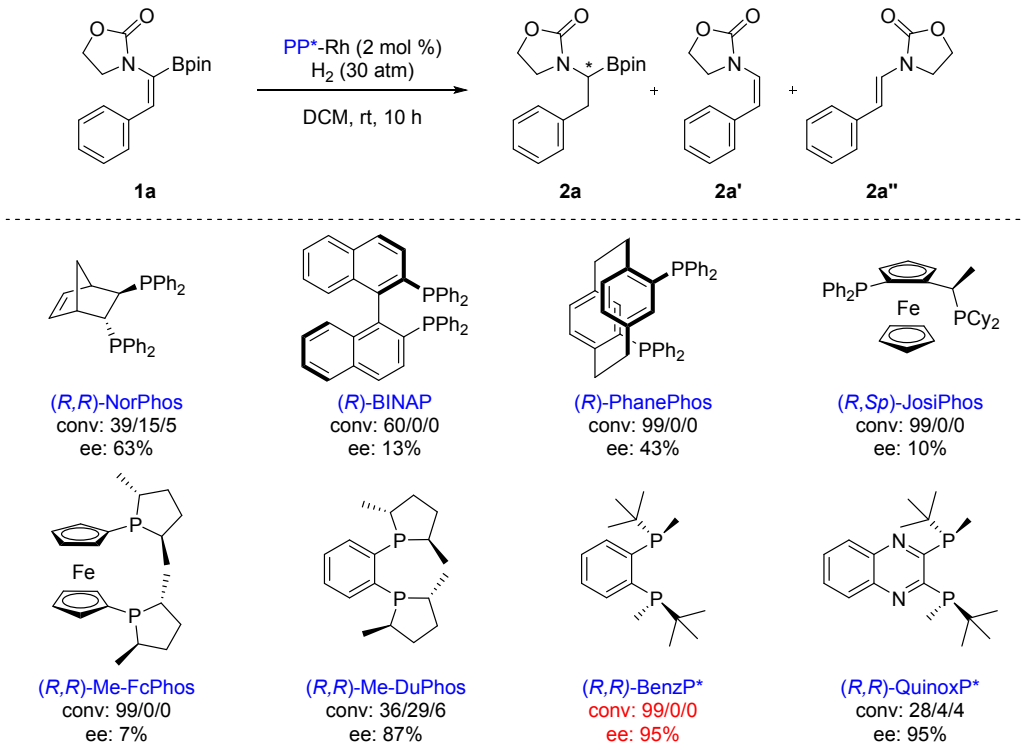

entry[a]	solvent	H_2 (atm)	conv 2a (%)[b]	ee (%)[c]
1	DCM	30	99	95
2	DCE	30	21	98
3	THF	30	87	94
4	DME	30	77	90
5	Toluene	30	77	98
6	EtOAc	30	99	96
7	EtOAc	20	99	96
8	EtOAc	5	99	96
9	EtOAc	1	26	96
10[d]	EtOAc	20	99	96

[a]Conditions: **1a** (0.1 mmol), PP*-Rh (2 mol %), H_2, solvent (2 mL), rt, 10 h, unless otherwise noted. [b]The conversions were calculated from ^{1}H-NMR spectra. [c]The ee values were determined by HPLC using chiral columns. [d][Rh((*R,R*)-BenzP*)(nbd)]SbF_6 (1 mol %).

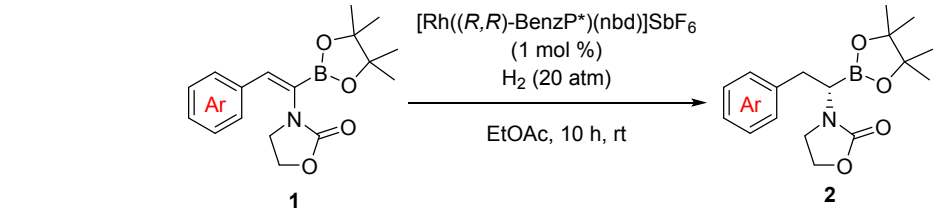

1 **2**

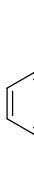

2a
98% yield, 96% ee

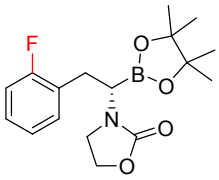

2b[a]
97% yield, 96% ee

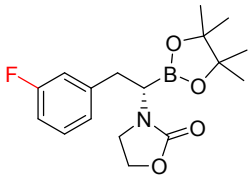

2c[a]
96% yield, 98% ee

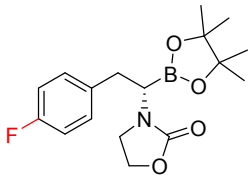

2d[a]
97% yield, 98% ee

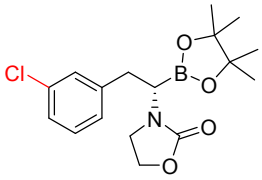

2e[c]
97% yield, 96% ee

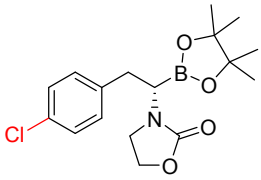

2f[b]
98% yield, 98% ee

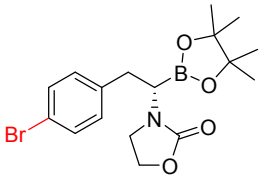

2g[a]
96% yield, 98% ee

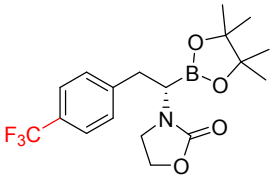

2h[a]
97% yield, 99% ee

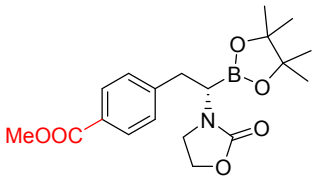

2i[a]
95% yield, 99% ee

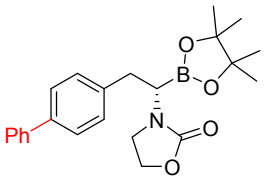

2j[a]
96% yield, 99% ee

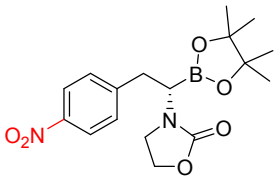

2k[a]
96% yield, 97% ee

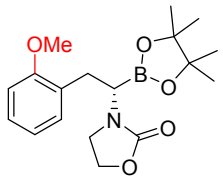

2l[c]
97% yield, 99% ee

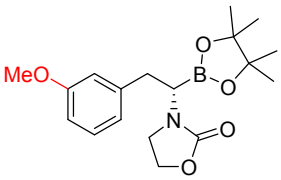

2m[c]
98% yield, 97% ee

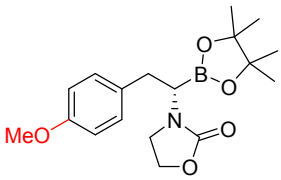

2n
96% yield, 92% ee

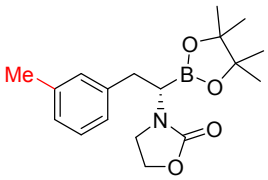

2o[a]
96% yield, 98% ee

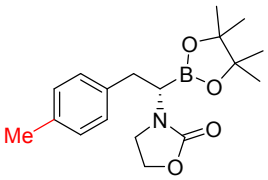

2p
97% yield, 97% ee

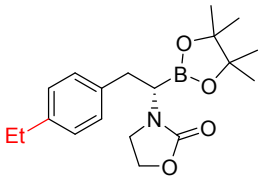

2q[b]
97% yield, 95% ee

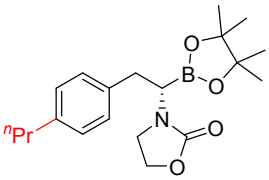

2r[a]
95% yield, 97% ee

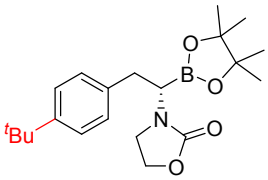

2s[a]
97% yield, 96% ee

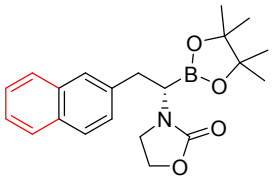

2t[b]
95% yield, 95% ee

Conditions: **1** (0.1 mmol), [Rh((*R*,*R*)-BenzP*)(nbd)]SbF_6 (1 mol %), H_2 (20 atm), EtOAc (2.0 mL), rt, 10 h, unless otherwise noted. Isolated yields. The ee values were determined by HPLC using chiral columns. [a][Rh((*R*,*R*)-BenzP*)(nbd)]SbF_6 (2 mol %), 24 h. [b]24 h. [c][Rh((*R*,*R*)-BenzP*)(nbd)]SbF_6 (4 mol %), 24 h.

Scheme 2. Substrate Scope.

the ee values of the desired chiral products were no less than 96% (**2b-g**). The substrates with trifluoromethyl, methoxy formyl, and phenyl groups at the *para*-position provided the products with complete conversions and almost perfect enantioselectivities (99% ee for **2h-j**), while another product **2k** with a nitro group at the *para*-position was obtained with 97% ee. When electron-donating groups such as methoxy and methyl were present at the *ortho*-, *meta*-, and *para*-positions, the activities increased while the enantioselectivities decreased gradually (**2l-p**). The activities of the catalytic reaction were reduced significantly when the *para*-substituent was changed from methyl to the relatively more bulky ethyl, *n*-propyl, and *t*-butyl groups, but the enantioselectivities were almost identical (**2q-s**). The naphthyl-substituted product **2t** can also be obtained in high yield and excellent enantioselectivity. To demonstrate the potential utilities of this protocol, the hydrogenation of **1a** was carried out on a gram scale using DCM as the solvent due to the solubility, affording the desired product in quantitative yield and with excellent enantioselectivity (Scheme 3).

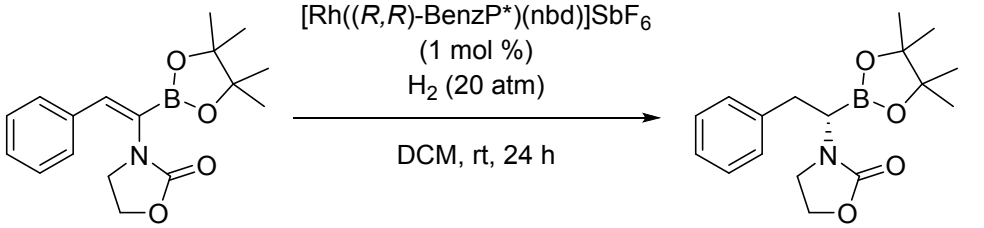

Scheme 3. Gram Scale Hydrogenation

To gain insight into the origin of activity and enantioselectivity, we have computed a catalytic cycle of the reaction (Scheme 4 and 5, Figure 3). Similarly to the catalytic cycles of other enamides, the amido group remains coordinated to the Rh atom throughout the whole catalytic cycle – either in a chelating or non-chelating way. Scheme 4 summarizes computations of the

hydrogen activation step. Although the solvate dihydrides **E** and **F** are reasonably stable, **TS1** and **TS2** have relatively high free energies, and the dihydride route for hydrogen activation is not the lowest energy pathway in this case. On the other hand, the chelated catalyst-substrate complexes **I** and **M** themselves are not capable of hydrogen activation. Molecular hydrogen complex **N** formed from the chelated **M**, rearranges to the gauche-coordinated[13d] molecular hydrogen complex **P** that can yield the monohydride **Q** with reasonably low barrier without intermediate formation of a dihydride. Monohydride **Q** can directly produce the hydrogenated product with the experimentally observed sense of enantioselection. However, the non-chelated complex **G**, formed as a result of the approaching hydrogen to the Rh atom in the chelated molecular hydrogen complex **J**, is significantly more reactive. Since the **TS4** (hydrogen activation via **K** and **L**) is also high in energy, apparently, all hydrogen activations proceed via **G** formed either from **J** or from the non-chelated catalyst-substrate complex **C**, yielding selectively the non-chelated dihydride intermediate **H**.

As shown in Scheme 5, barrierless coordination of the double bond in **H** can give either α- or β-dihydride **R** and **S**, respectively. The following migratory insertion and reductive elimination proceed faster starting from **S** thus providing selective formation of the *S*-product. Therefore, the *S* enantioselectivity is determined by the difference in stabilities of **TS3** (-6.2 kcal/mol) and **TS4** (-2.0 kcal/mol) which halves the number of possible pathways in the late reaction stages, as well as between **TS6** (-14.5 kcal/mol) and **TS7** (-11.3 kcal/mol) that secures the formation of the *S*-product.

Notably, in both cases the relative stability of **TS3** or **TS6** is caused by the pinacolylboryl group being in close proximity to the *t*-Bu group, leading to the significant energy difference (Figure 3). Thus, in **TS3**, the phenyl group is not participating in any intramolecular interactions.

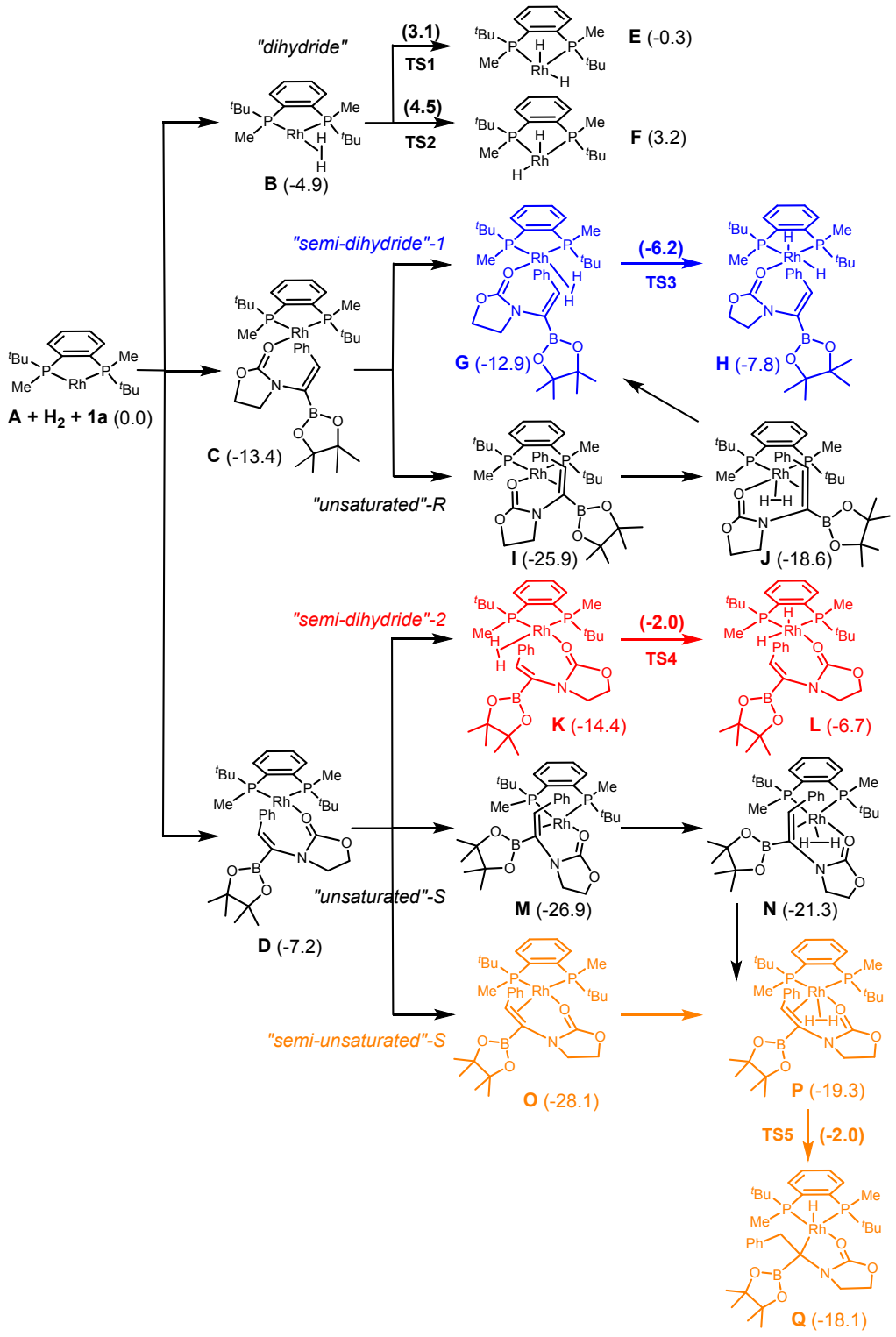

Scheme 4. Calculated Free Energies for Hydrogen Activation via Various Pathways (A positive charge on each Rh atom is omitted for clarity. The unit of energies is kcal/mol.)

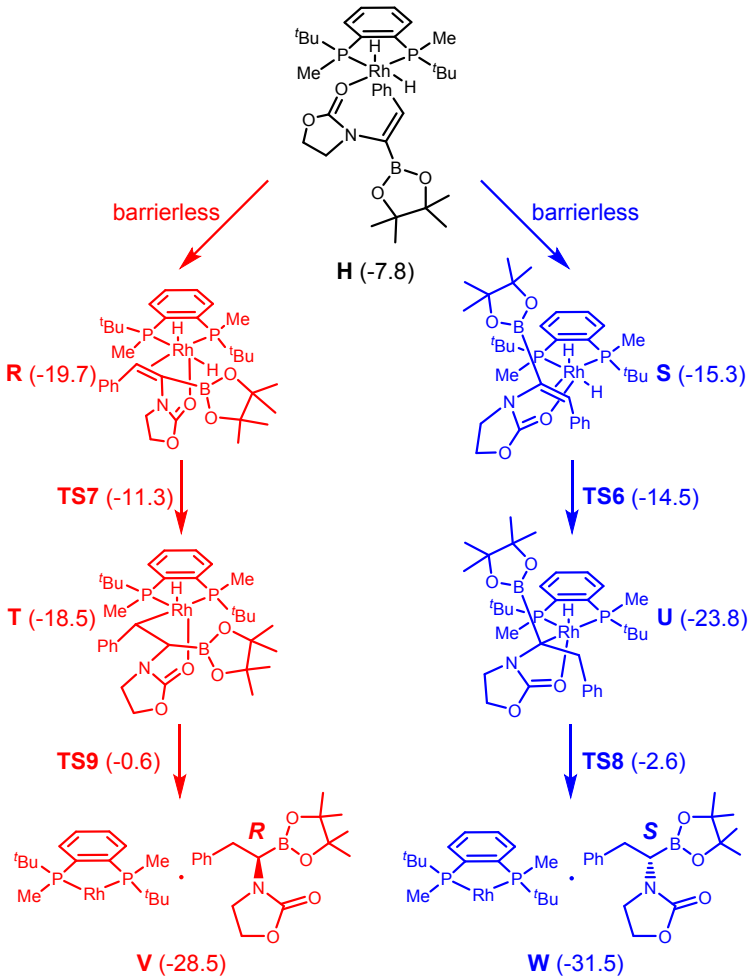

Scheme 5. Calculated Free Energies for Hydrogen Transfer of Alternative Pathways (A positive charge on each Rh atom is omitted for clarity. The unit of energies is kcal/mol.)

In the same fashion, in **TS4**, only the C-H···π interaction between the methyl group of the ligand and the phenyl group of the substrate participates in the stabilization of the transition state. Hence, the stabilizing free energy provided by the nonbonding interaction of *t*-Bu and pinacoylboryl groups can be estimated to be over 4 kcal/mol. Comparing **TS6** and **TS7**, it is difficult to make any similar semi-quantitative estimation. It is only clear that the stabilizing nonbonding interactions in **TS6** are significantly greater in number than those in **TS7**, and that the contribution from the *t*-Bu···Bpin interaction is likely to also be around 4 kcal/mol.[15] We are

convinced that accumulation of the knowledge on the strength of the nonbonding interaction between various groups provides useful information for the construction of potential substrates and catalysts for asymmetric catalytic transformations.

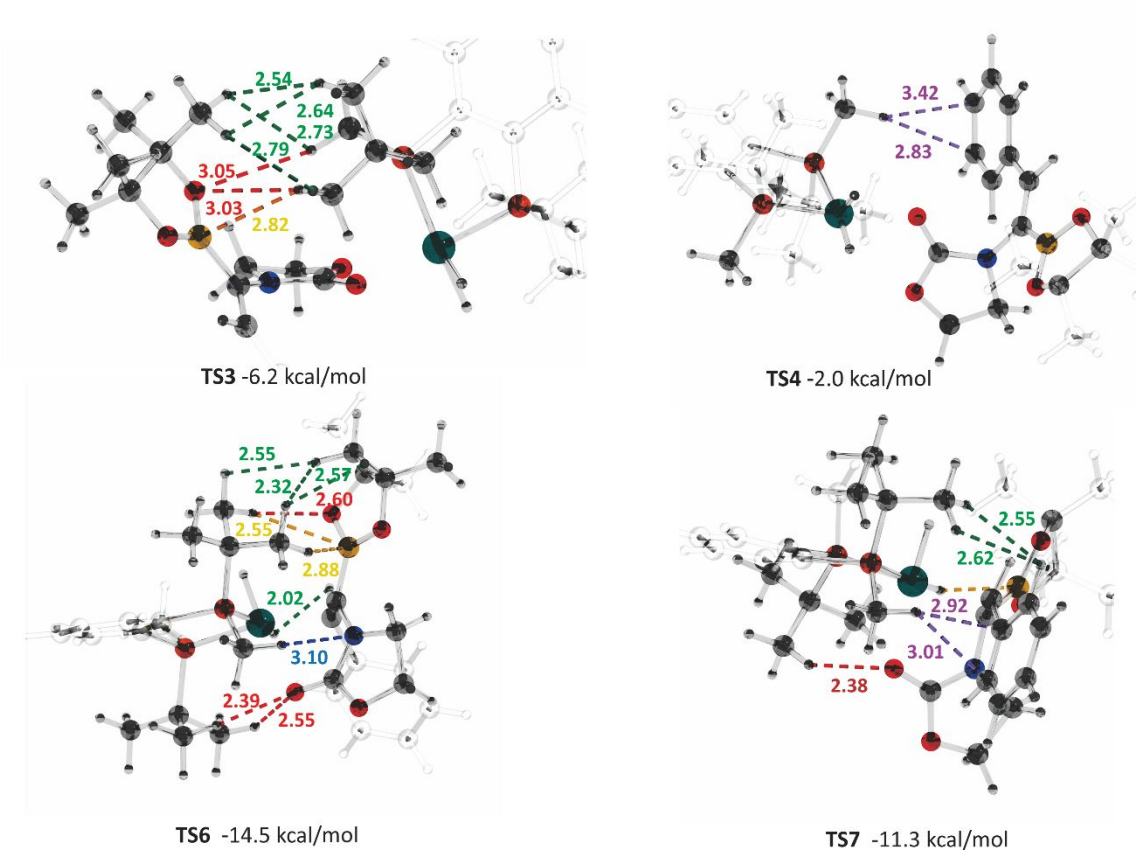

Figure 3. Optimized structures of **TS3** and **TS4** (up); **TS6** and **TS7** (down), their relative Gibbs free energies and interatomic distances (Angstroms) for intramolecular interactions: C-H···H-C (green), C-H···O (red), C-H···π (violet), C-H···B (yellow), and C-H···N (blue).[16] Significant relative stability of **TS6** is secured by the whole network of 10 interactions against only 5 in **TS7**.

■ CONCLUSIONS

In summary, we have developed a highly efficient route for the synthesis of chiral α-aminoboronates in high yield and excellent enantioselectivity via the rhodium-catalyzed

asymmetric hydrogenation of α-boryl enamides. Computational studies showed that nonbonding interactions of *t*-Bu···Bpin are important for both reactivity and selectivity. In addition, the catalytic reaction can be carried out on a gram scale without any loss in enantioselectivity.

■ EXPERIMENTAL SECTION

[Rh((*R*,*R*)-BenzP*)(nbd)]SbF_6 (0.001 mmol) and substrate (0.1 mmol) were placed in a hydrogenation tube and then charged in an autoclave. The system was evacuated and filled with hydrogen. After repeating this operation 3 times, degassed EtOAc (2 mL) was added and the hydrogen pressure was adjusted to 20 atm. After vigorous stirring at room temperature for 10 h, the vessel was vented and the reaction mixture was evaporated under reduced pressure. The conversation was calculated from the ^{1}H NMR spectrum of the crude product. After purification by column chromatography, the enantiomeric excess of the product was determined by HPLC using a chiral column.

■ AUTHOR INFORMATION

Corresponding Author

*E-mail: wanbin@sjtu.edu.cn

*E-mail: gridnev.ilya.a6@tohoku.ac.jp

*E-mail: zhenfeng@sjtu.edu.cn

Notes

The authors declare no competing financial interest.

■ ASSOCIATED CONTENT

Supporting Information

The Supporting Information is available free of charge on the ACS Publications website at DOI:

Synthetic details for substrates, procedures for hydrogenation reactions, spectra of NMR and HPLC data, computational details (PDF)

Crystallographic data for **2h** (CIF)

■ ACKNOWLEDGMENTS

This work was supported by National Key R&D Program of China (No. 2018YFE0126800), National Natural Science Foundation of China (Nos. 21620102003, 21831005, 91856106, and 21572131), and Shanghai Municipal Education Commission (No. 201701070002E00030). We thank the Instrumental Analysis Center of Shanghai Jiao Tong University. We acknowledge the generous gifts of the P-stereogenic bisphosphine ligands from Nippon Chemical Industrial Co. Ltd.

■ REFERENCES

(1) (a) Brooks, W. L. A.; Sumerlin, B. S. Synthesis and Applications of Boronic Acid-Containing Polymers: From Materials to Medicine. *Chem. Rev.* **2016**, *116*, 1375–1397. (b) Fyfe, J. W. B.; Watson, A. J. B. Recent Developments in Organoboron Chemistry: Old Dogs, New Tricks. *Chem* **2017**, *3*, 31–55. (c) Akgun, B.; Hall, D. G. Boronic Acids as Bioorthogonal Probes for Site-Selective Labeling of Proteins. *Angew. Chem. Int. Ed.* **2018**, *57*, 13028–13044. (d) Namirembe, S.; Morken, J. P. Reactions of Organoboron Compounds Enabled by Catalyst-Promoted Metalate Shifts. *Chem. Soc. Rev.* **2019**, *48*, 3464–3474. (e) Hall, D. G. Boronic Acid Catalysis. *Chem. Soc. Rev.* **2019**, *48*, 3475–3496. (f) António, J. P. M.; Russo, R.; Carvalho, C. P.; Cal, P. M. S. D.; Gois, P. M. P. Boronic Acids as Building Blocks for the Construction of Therapeutically Useful Bioconjugates. *Chem. Soc. Rev.* **2019**. *48*, 3513-3536. (g) Mellerup, S. K.; Wang, S. Boron-Based Stimuli Responsive Materials. *Chem. Soc. Rev.* **2019**, *48*, 3537–3549.

(h) Lam, J.; Szkop, K. M.; Mosaferi, E.; Stephan, D. W. FLP Catalysis: Main Group Hydrogenations of Organic Unsaturated Substrates. *Chem. Soc. Rev.* **2019**, *48*, 3592–3612. (i) Su, Y.; Kinjo, R. Small Molecule Activation by Boron-Containing Heterocycles. C*hem. Soc. Rev.* **2019**. *48*, 3613–3659.

(2) Reviews: (a) Matteson, D. S. Boronic Esters in Asymmetric Synthesis. *J. Org. Chem.* **2013**, *78*, 10009–10023. (b) Collins, B. S. L.; Wilson, C. M.; Myers, E. L.; Aggarwal, V. K. Asymmetric Synthesis of Secondary and Tertiary Boronic Esters. *Angew. Chem. Int. Ed.* **2017**, *56*, 11700–11733. (c) Quan, M.; Wu, L.; Yang, G.; Zhang, W. Pd(II), Ni(II) and Co(II)-Catalyzed Enantioselective Additions of Organoboron Reagents to Ketimines. *Chem. Commun.* **2018**, *54*, 10394–10404. (d) Yang, X.; Kalita, S. J.; Maheshuni, S.; Huang, Y.-Y. Recent Advances on Transition-Metal-Catalyzed Asymmetric Tandem Reactions with Organoboron Reagents. *Coord. Chem. Rev.* **2019**, *392*, 35–48. Recent papers: (e) Shoba, V. M.; Thacker, N. C.; Bochat, A. J.; Takacs, J. M. Synthesis of Chiral Tertiary Boronic Esters by Oxime-Directed Catalytic Asymmetric Hydroboration. *Angew. Chem. Int. Ed.* **2016**, *55*, 1465–1469. (f) Schmidt, J.; Choi, J.; Liu, A. T.; Slusarczyk, M.; Fu, G. C. A General, Modular Method for the Catalytic Asymmetric Synthesis of Alkylboronate Esters. *Science* **2016**, *354*, 1265–1270. (g) Chakrabarty, S.; Takacs, J. M. Synthesis of Chiral Tertiary Boronic Esters: Phosphonate-Directed Catalytic Asymmetric Hydroboration of Trisubstituted Alkenes. *J. Am. Chem. Soc.* **2017**, *139*, 6066–6069. (h) Myhill, J. A.; Zhang, L.; Lovinger, G. J.; Morken, J. P. Enantioselective Construction of Tertiary Boronic Esters by Conjunctive Cross-Coupling. *Angew. Chem. Int. Ed.* **2018**, *57*, 12799–12803. (i) Tao, Z.; Robb, K. A.; Panger, J. L.; Denmark, S. E. Enantioselective, Lewis Base-Catalyzed Carbosulfenylation of Alkenylboronates by 1,2-Boronate Migration. *J. Am. Chem. Soc.* **2018**, *140*, 15621–15625.

(3) Reviews: (a) Georgiou, I.; Ilyashenko, G.; Whiting, A. Synthesis of Aminoboronic Acids and Their Applications in Bifunctional Catalysis. *Acc. Chem. Res.* **2009**, *42*, 756–768. (b) Touchet, S.; Carreaux, F.; Carboni, B.; Bouillon, A.; Boucher, J.-L. Aminoboronic Acids and Esters: From Synthetic Challenges to the Discovery of Unique Classes of Enzyme Inhibitors. *Chem. Soc. Rev.* **2011**, *40*, 3895–3914. (c) Smoum, R.; Rubinstein, A.; Dembitsky, V. M.; Srebnik, M. Boron Containing Compounds as Protease Inhibitors. *Chem. Rev.* **2012**, *112*, 4156–4220. (d) Andrés, P.; Ballano, G.; Calaza, M. I.; Cativiela, C. Synthesis of α-Aminoboronic Acids. *Chem. Soc. Rev.* **2016**, *45*, 2291–2307. (e) Šterman, A.; Sosič, I.; Gobec, S.; Časar, Z. Synthesis of Aminoboronic Acid Derivatives: An Update on Recent Advances. *Org. Chem. Front.* **2019**, *6*, 2991–2998. Representative papers: (f) Winkler, M. L.; Rodkey, E. A.; Taracila, M. A.; Drawz, S. M.; Bethel, C. R.; Papp-Wallace, K. M.; Smith, K. M.; Xu, Y.; Dwulit-Smith, J. R.; Romagnoli, C.; Caselli, E.; Prati, F.; van den Akker, F.; Bonomo, R. A. Design and Exploration of Novel Boronic Acid Inhibitors Reveals Important Interactions with a Clavulanic Acid-Resistant Sulfhydryl-Variable (SHV) β-Lactamase. *J. Med. Chem.* **2013**, *56*, 1084–1097. (g) Poplawski, S. E.; Lai, J. H.; Li, Y.; Jin, Z.; Liu, Y.; Wu, W.; Wu, Y.; Zhou, Y.; Sudmeier, J. L.; Sanford, D. G.; Bachovchin, W. W. Identification of Selective and Potent Inhibitors of Fibroblast Activation Protein and Prolyl Oligopeptidase. *J. Med. Chem.* **2013**, *56*, 3467–3477. (h) Kawamura, S.; Unno, Y.; Asai, A.; Arisawa, M.; Shuto, S. Structurally Novel Highly Potent Proteasome Inhibitors Created by the Structure-Based Hybridization of Nonpeptidic Belactosin Derivatives and Peptide Boronates. *J. Med. Chem.* **2014**, *57*, 2726–2735. (i) Caselli, E.; Romagnoli, C.; Vahabi, R.; Taracila, M. A.; Bonomo, R. A.; Prati, F. Click Chemistry in Lead Optimization of Boronic Acids as β-Lactamase Inhibitors. *J. Med. Chem.* **2015**, *58*, 5445–5458. (j) Chu, Q.; Diedrich, J. K.; Vaughan, J. M.; Donaldson, C. J.; Nunn, M. F.; Lee, K.-F.;

Saghatelian, A. HtrA1 Proteolysis of ApoE In Vitro Is Allele Selective. *J. Am. Chem. Soc.* **2016**, *138*, 9473–9478. (k) Nitsche, C.; Zhang, L.; Weigel, L. F.; Schilz, J.; Graf, D.; Bartenschlager, R.; Hilgenfeld, R.; Klein, C. D. Peptide-Boronic Acid Inhibitors of Flaviviral Proteases: Medicinal Chemistry and Structural Biology. *J. Med. Chem.* **2017**, *60*, 511–516. (l) Diaz, D. B.; Yudin, A. K. The Versatility of Boron in Biological Target Engagement. *Nat. Chem.* **2017**, *9*, 731–742. (m) Xie, S. C.; Gillett, D. L.; Spillman, N. J.; Tsu, C.; Luth, M. R.; Ottilie, S.; Duffy, S.; Gould, A. E.; Hales, P.; Seager, B. A.; Charron, C. L.; Bruzzese, F.; Yang, X.; Zhao, X.; Huang, S.-C.; Hutton, C. A.; Burrows, J. N.; Winzeler, E. A.; Avery, V. M.; Dick, L. R.; Tilley, L. Target Validation and Identification of Novel Boronate Inhibitors of the Plasmodium Falciparum Proteasome. *J. Med. Chem.* **2018**, *61*, 10053–10066.

(4) (a) Matteson, D. S.; Sadhu, K. M.; Lienhard, G. E. (*R*)-1-Acetamido-2-phenylethaneboronic Acid. A Specific Transition-State Analogue for Chymotrypsin. *J. Am. Chem. Soc.* **1981**, *103*, 5241–5242. (b) Matteson, D. S. α-Amido Boronic Acids: A Synthetic Challenge and Their Properties as Serine Protease Inhibitors. *Med. Res. Rev.* **2008**, *28*, 233–246. (c) Beenen, M. A.; An, C.; Ellman, J. A. Asymmetric Copper-Catalyzed Synthesis of α-Amino Boronate Esters from *N*-*tert*-Butanesulfinyl Aldimines. *J. Am. Chem. Soc.* **2008**, *130*, 6910–6911. (d) He, Z.; Zajdlik, A.; St. Denis, J. D.; Assem, N.; Yudin, A. K. Boroalkyl Group Migration Provides a Versatile Entry into α-Aminoboronic Acid Derivatives. *J. Am. Chem. Soc.* **2012**, *134*, 9926–9929. (e) Wen, K.; Wang, H.; Chen, J.; Zhang, H.; Cui, X.; Wei, C.; Fan, E.; Sun, Z. Improving Carbene-Copper-Catalyzed Asymmetric Synthesis of α-Aminoboronic Esters Using Benzimidazole-Based Precursors. *J. Org. Chem.* **2013**, *78*, 3405–3409. (f) Wen, K.; Chen, J.; Gao, F.; Bhadury, P. S.; Fan, E.; Sun, Z. Metal Free Catalytic Hydroboration of Multiple Bonds in Methanol Using *N*-Heterocyclic Carbenes under Open Atmosphere. *Org. Biomol.*

Chem. **2013**, *11*, 6350–6356. (g) Xie, J.-b; Luo, J.; Winn, T. R.; Cordes, D. B.; Li, G. Group-Assisted Purification (GAP) Chemistry for the Synthesis of Velcade via Asymmetric Borylation of *N*-Phosphinylimines. *Beilstein J. Org. Chem.* **2014**, *10*, 746–751. (h) Buesking, A. W.; Bacauanu, V.; Cai, I.; Ellman, J. A. Asymmetric Synthesis of Protected α-Amino Boronic Acid Derivatives with an Air- and Moisture-Stable Cu(II) Catalyst. *J. Org. Chem.* **2014**, *79*, 3671–3677. (i) Chen, J.; Chen, L.-y.; Zheng, Y.; Sun, Z. Asymmetric Synthesis of Stable α-Aminoboronic Esters Catalyzed by *N*-Heterocylic Carbene and Copper(I) Chloride. *RSC Adv.* **2014**, *4*, 21131–21133. (j) Li, C.; Wang, J.; Barton, L. M.; Yu, S.; Tian, M.; Peters, D. S.; Kumar, M.; Yu, A. W.; Johnson, K. A.; Chatterjee, A. K.; Yan, M; Baran P. S. Decarboxylative Borylation. *Science* **2017**, *356,* eaam7335.

(5) (a) Batsanov, A. S.; Grosjean, C.; Schütz, T.; Whiting, A. A (-)-Sparteine-Directed Highly Enantioselective Synthesis of Boroproline. Solid- and Solution-State Structure and Properties. *J. Org. Chem.* **2007**, *72*, 6276–6279. (b) Qi, Q.; Yang, X.; Fu, X.; Xu, S.; Negishi, E.-i. Highly Enantiospecific Borylation for Chiral α-Amino Tertiary Boronic Esters. *Angew. Chem. Int. Ed.* **2018**, *57*, 15138–15142.

(6) (a) Solé, C.; Gulyás, H.; Fernández, E. Asymmetric Synthesis of α-Amino Boronate Esters via Organocatalytic Pinacolboryl Addition to Tosylaldimines. *Chem. Commun.* **2012**, *48*, 3769–3771. (b) Zhang, S.-S.; Zhao, Y.-S.; Tian, P.; Lin, G.-Q. Chiral NHC/Cu(I)-Catalyzed Asymmetric Hydroboration of Aldimines: Enantioselective Synthesis of α-Amido Boronic Esters. *Synlett* **2013**, *24*, 437–442. (c) Hong, K.; Morken, J. P. Catalytic Enantioselective One-Pot Aminoborylation of Aldehydes: A Strategy for Construction of Nonracemic α-Amino Boronates. *J. Am. Chem. Soc.* **2013**, *135*, 9252–9254. (d) Hu, N.; Zhao, G.; Zhang, Y.; Liu, X.; Li, G.; Tang, W. Synthesis of Chiral α-Amino Tertiary Boronic Esters by Enantioselective

Hydroboration of α-Arylenamides. *J. Am. Chem. Soc.* **2015**, *137*, 6746–6749. (e) Wang, D.; Cao, P.; Wang, B.; Jia, T.; Lou, Y.; Wang, M.; Liao, J. Copper(I)-Catalyzed Asymmetric Pinacolboryl Addition of *N*-Boc-Imines Using a Chiral Sulfoxide-Phosphine Ligand. *Org. Lett.* **2015**, *17*, 2420–2423. (f) Chen, L.; Zou, X.; Zhao, H.; Xu, S. Copper-Catalyzed Asymmetric Protoboration of β-Amidoacrylonitriles and β-Amidoacrylate Esters: An Efficient Approach to Functionalized Chiral α-Amino Boronate Esters. *Org. Lett.* **2017**, *19*, 3676–3679. (g) López, A.; Clark, T. B.; Parra, A.; Tortosa, M. Copper-Catalyzed Enantioselective Synthesis of β-Boron β-Amino Esters. *Org. Lett.* **2017**, *19*, 6272–6275. (h) Schwamb, C. B.; Fitzpatrick, K. P.; Brueckner, A. C.; Richardson, H. C.; Cheong, P. H.-Y.; Scheidt, K. A. Enantioselective Synthesis of α-Amidoboronates Catalyzed by Planar-Chiral NHC-Cu(I) Complexes. *J. Am. Chem. Soc.* **2018**, *140*, 10644–10648. (i) Chen, L.; Shen, J.-J.; Gao, Q.; Xu, S. Synthesis of Cyclic Chiral α-Amino Boronates by Copper-Catalyzed Asymmetric Dearomative Borylation of Indoles. *Chem. Sci.* **2018**, *9*, 5855–5859.

(7) (a) Nishikawa, D.; Hirano, K.; Miura, M. Asymmetric Synthesis of α-Aminoboronic Acid Derivatives by Copper-Catalyzed Enantioselective Hydroamination. *J. Am. Chem. Soc.* **2015**, *137*, 15620–15623. (b) Nishikawa, D.; Hirano, K.; Miura, M. Copper-Catalyzed Regio- and Stereoselective Aminoboration of Alkenylboronates. *Org. Lett.* **2016**, *18*, 4856–4859.

(8) Reviews: (a) Xie, J.-H.; Zhu, S.-F.; Zhou, Q.-L. Transition Metal-Catalyzed Enantioselective Hydrogenation of Enamines and Imines. *Chem. Rev.* **2011**, 1713–1760. (b) Wang, D.-S.; Chen, Q.-A.; Lu, S.-M.; Zhou, Y.-G. Asymmetric Hydrogenation of Heteroarenes and Arenes. *Chem. Rev.* **2012**, *112*, 2557–2590. (c) Chen, Q.-A.; Ye, Z.-S.; Duan, Y.; Zhou, Y.-G. Homogeneous Palladium-Catalyzed Asymmetric Hydrogenation. *Chem. Soc. Rev.* **2013**, *42*, 497–511. (d) Verendel, J. J.; Pàmies, O.; Diéguez, M.; Andersson, P. G. Asymmetric

Hydrogenation of Olefins Using Chiral Crabtree-Type Catalysts: Scope and Limitations. *Chem. Rev.* **2014**, *114*, 2130–2169. (e) Zhang, Z.; Butt, N. A.; Zhang, W. Asymmetric Hydrogenation of Nonaromatic Cyclic Substrates. *Chem. Rev.* **2016**, *116*, 14769–14821. (f) Zhang, Z.; Butt, N. A.; Zhou, M.; Liu, D.; Zhang, W. Asymmetric Transfer and Pressure Hydrogenation with Earth-Abundant Transition Metal Catalysts. *Chin. J. Chem.* **2018**, *36*, 443–454. Recent papers: (g) Friedfeld, M. R.; Zhong, H.; Ruck, R. T.; Shevlin, M.; Chirik, P. J. Cobalt-Catalyzed Asymmetric Hydrogenation of Enamides Enabled by Single-Electron Reduction. *Science* **2018**, *360*, 888–893. (h) Yan, Q.; Xiao, G.; Wang, Y.; Zi, G.; Zhang, Z.; Hou, G. Highly Efficient Enantioselective Synthesis of Chiral Sulfones by Rh-Catalyzed Asymmetric Hydrogenation. *J. Am. Chem. Soc.* **2019**, *141*, 1749–1756. (i) Chen, Y.; He, Y.-M.; Zhang, S.; Miao, T.; Fan, Q.-H. Rapid Construction of Structurally Diverse Quinolizidines, Indolizidines, and Their Analogues via Ruthenium-Catalyzed Asymmetric Cascade Hydrogenation/Reductive Amination. *Angew. Chem. Int. Ed.* **2019**, *58*, 3809–3813. (j) Zhang, L.; Tang, Y.; Han, Z.; Ding, K. Lutidine-Based Chiral Pincer Manganese Catalysts for Enantioselective Hydrogenation of Ketones. *Angew. Chem. Int. Ed.* **2019**, *58*, 4973–4977. (k) Li, C.; Wan, F.; Chen, Y.; Peng, H.; Tang, W.; Yu, S.; McWilliams, J. C.; Mustakis, J.; Samp, L.; Maguire, R. J. Stereoelectronic Effects in Ligand Design: Enantioselective Rhodium-Catalyzed Hydrogenation of Aliphatic Cyclic Tetrasubstituted Enamides and Concise Synthesis of (*R*)-Tofacitinib. *Angew. Chem. Int. Ed.* **2019**, *58*, 13573–13583. (l) You, C.; Li, X.; Gong, Q.; Wen, J.; Zhang, X. Nickel-Catalyzed Desymmetric Hydrogenation of Cyclohexadienones: An Efficient Approach to All-Carbon Quaternary Stereocenters. *J. Am. Chem. Soc.* **2019**, *141*, 14560–14564.

(9) Representative papers: (a) Gridnev, I. D.; Higashi, N.; Imamoto, T. Interconversion of Monohydride Intermediates in Rh(I)-Catalyzed Asymmetric Hydrogenation of Dimethyl 1-

Benzoyloxyethenephosphonate. *J. Am. Chem. Soc.* **2001**, *123*, 4631–4632. (b) Tang, W.; Zhang, X. A Chiral 1,2-Bisphospholane Ligand with a Novel Structural Motif: Applications in Highly Enantioselective Rh-Catalyzed Hydrogenations. *Angew. Chem. Int. Ed.* **2002**, *41*, 1612–1614. (c) Tang, W.; Wang, W.; Chi, Y.; Zhang, X. A Bisphosphepine Ligand with Stereogenic Phosphorus Centers for the Practical Synthesis of β-Aryl-β-Amino Acids by Asymmetric Hydrogenation. *Angew. Chem. Int. Ed.* **2003**, *42*, 3509–3511. (d) Hoge, G.; Wu, H.-P.; Kissel, W. S.; Pflum, D. A.; Greene, D. J.; Bao, J. Highly Selective Asymmetric Hydrogenation Using a Three Hindered Quadrant Bisphosphine Rhodium Catalyst. *J. Am. Chem. Soc.* **2004**, *126*, 5966–5967. (e) Liu, Y.; Ding, K. Modular Monodentate Phosphoramidite Ligands for Rhodium-Catalyzed Enantioselective Hydrogenation. *J. Am. Chem. Soc.* **2005**, *127*, 10488–10489. (f) Imamoto, T.; Sugita, K.; Yoshida, K. An Air-Stable P-Chiral Phosphine Ligand for Highly Enantioselective Transition-Metal-Catalyzed Reactions. *J. Am. Chem. Soc.* **2005**, *127*, 11934–11935. (g) Zhang, X.; Huang, K.; Hou, G.; Cao, B.; Zhang, X. Electron-Donating and Rigid P-Stereogenic Bisphospholane Ligands for Highly Enantioselective Rhodium-Catalyzed Asymmetric Hydrogenations. *Angew. Chem. Int. Ed.* **2010**, *49*, 6421–6424. (h) Revés, M.; Ferrer, C.; León, T.; Doran, S.; Etayo, P.; Vidal-Ferran, A.; Riera, A.; Verdaguer, X. Primary and Secondary Aminophosphines as Novel P-Stereogenic Building Blocks for Ligand Synthesis. *Angew. Chem. Int. Ed.* **2010**, *49*, 9452–9455. (i) Ager, D. J.; de Vries, A. H. M.; de Vries, J. G. Asymmetric Homogeneous Hydrogenations at Scale. *Chem. Soc. Rev.* **2012**, *41*, 3340–3380. (j) Molinaro, C.; Scott, J. P.; Shevlin, M.; Wise, C.; Ménard, A.; Gibb, A.; Junker, E. M.; Lieberman, D. Catalytic, Asymmetric, and Stereodivergent Synthesis of Non-Symmetric β,β-Diaryl-α-amino Acids. *J. Am. Chem. Soc.* **2015**, *137*, 999–1006.

(10) (a) Wollenburg, M.; Moock, D.; Glorius, F. Hydrogenation of Borylated Arenes. *Angew. Chem. Int. Ed.* **2019**, *58*, 6549–6553. (b) Ling, L.; He, Y.; Zhang, X.; Luo, M.; Zeng, X. Hydrogenation of (Hetero)aryl Boronate Esters with a Cyclic (Alkyl)(amino)carbene–Rhodium Complex: Direct Access to *cis*-Substituted Borylated Cycloalkanes and Saturated Heterocycles. *Angew. Chem. Int. Ed.* **2019**, *58*, 6554–6558.

(11) (a) Chen, J.; Zhang, Z.; Li, B.; Li, F.; Wang, Y.; Zhao, M.; Gridnev, I. D.; Imamoto, T.; Zhang, W. Pd(OAc)2-Catalyzed Asymmetric Hydrogenation of Sterically Hindered *N*-Tosylimines. *Nat. Commun.* **2018**, *9*, 5000. (b) Fan, D.; Liu, Y.; Jia, J.; Zhang, Z.; Liu, Y.; Zhang, W. Synthesis of Chiral α-Aminosilanes through Palladium-Catalyzed Asymmetric Hydrogenation of Silylimines. *Org. Lett.* **2019**, *21*, 1042–1045. (c) Li, B.; Chen, J.; Zhang, Z.; Gridnev, I. D.; Zhang, W. Nickel-Catalyzed Asymmetric Hydrogenation of *N*-Sulfonyl Imines. *Angew. Chem. Int. Ed.* **2019**, *58*, 7329–7334. (d) Zhang, J.; Jia, J.; Zeng, X.; Wang, Y.; Zhang, Z.; Gridnev, I. D.; Zhang, W. Chemo- and Enantioselective Hydrogenation of α-Formyl Enamides: An Efficient Access to Chiral α-Amido Aldehydes. *Angew. Chem. Int. Ed.* **2019**, *58*, 11505–11512. (e) Hu, Y.; Zhang, Z.; Zhang, J.; Liu, Y.; Gridnev, I. D.; Zhang, W. Cobalt-Catalyzed Asymmetric Hydrogenation of C=N Bonds Enabled by Assisted Coordination and Nonbonding Interactions. *Angew. Chem. Int. Ed.* **2019**, *58*, 15767–15771.

(12) (a) Liu, Y.; Zhang, W. Iridium-Catalyzed Asymmetric Hydrogenation of α-Alkylidene Succinimides. *Angew. Chem. Int. Ed.* **2013**, *52*, 2203–2206. (b) Chen, J.; Liu, D.; Butt, N.; Li, C.; Fan, D.; Liu, Y.; Zhang, W. Palladium-Catalyzed Asymmetric Hydrogenation of α-Acyloxy-1- Arylethanones. *Angew. Chem. Int. Ed.* **2013**, *52*, 11632–11636. (c) Liu, Y.; Gridnev, I. D.; Zhang, W. Mechanism of the Asymmetric Hydrogenation of Exocyclic α,β-Unsaturated Carbonyl Compounds with an Iridium/BiphPhox Catalyst: NMR and DFT Studies. *Angew. Chem.*

Int. Ed. **2014**, *53*, 1901–1905. (d) Hu, Q.; Zhang, Z.; Liu, Y.; Imamoto, T.; Zhang, W. $ZnCl_2$-Promoted Asymmetric Hydrogenation of β-Secondary-Amino Ketones Catalyzed by a P-Chiral Rh-Bisphosphine Complex. *Angew. Chem. Int. Ed.* **2015**, *54*, 2260–2264. (e) Zhang, Z.; Hu, Q.; Wang, Y.; Chen, J.; Zhang, W. Rh-Catalyzed Asymmetric Hydrogenation of Cyclic α-Dehydroamino Ketones. *Org. Lett.* **2015**, *17*, 5380–5383. (f) Chen, J.; Zhang, Z.; Liu, D.; Zhang, W. Palladium-Catalyzed Chemo- and Enantioselective C−O Bond Cleavage of α-Acyloxy Ketones by Hydrogenolysis. *Angew. Chem. Int. Ed.* **2016**, *55*, 8444–8447. (g) Hu, Q.; Chen, J.; Zhang, Z.; Liu, Y.; Zhang, W. Rh-Catalyzed One-Pot Sequential Asymmetric Hydrogenation of α-Dehydroamino Ketones for the Synthesis of Chiral Cyclic *trans*-β-Amino Alcohols. *Org. Lett.* **2016**, *18*, 1290–1293. (h) Hu, Q.; Hu, Y.; Liu, Y.; Zhang, Z.; Liu, Y.; Zhang, W. Rh-Catalyzed Chemo- and Enantioselective Hydrogenation of Allylic Hydrazones. *Chem. Eur. J.* **2017**, *23*, 1040–1043. (i) Liu, C.; Yuan, J.; Zhang, J.; Wang, Z.; Zhang, Z.; Zhang, W. Rh-Catalyzed Asymmetric Hydrogenation of β-Branched Enol Esters for the Synthesis of β-Chiral Primary Alcohols. *Org. Lett.* **2018**, *20*, 108–111. (j) Zhang, J.; Liu, C.; Wang, X.; Chen, J.; Zhang, Z.; Zhang, W. Rhodium-Catalyzed Asymmetric Hydrogenation of β-Branched Enamides for the Synthesis of β-Stereogenic Amines. *Chem. Commun.* **2018**, *54*, 6024–6027. (k) Jia, J.; Ling, Z.; Zhang, Z.; Tamura, K.; Gridnev, I. D.; Imamoto, T.; Zhang, W. An Atropos Chiral Biphenyl Bisphosphine Ligand Bearing Only 2,2′-Substituents and Its Application in Rh-Catalyzed Asymmetric Hydrogenation. *Adv. Synth. Catal.* **2018**, *360*, 738–743. (l) Fan, D.; Hu, Y.; Jiang, F.; Zhang, Z.; Zhang, W. Rhodium-Catalyzed Chemo- and Enantioselective Hydrogenation of Alkynyl-Aryl Hydrazones. *Adv. Synth. Catal.* **2018**, *360*, 2228–2232.

(13) (a) Miura, T.; Imamoto, T. Enantiomerically Pure 1,2-Bis(Isopropylmethylphosphino) Benzene and Its Use in Highly Enantioselective Rh-Catalyzed Asymmetric Hydrogenation.

Tetrahedron Lett. **1999**, *40*, 4833–4836. (b) Yamamoto, Y.; Koizumi, T.; Katagiri, K.; Furuya, Y.; Danjo, H.; Imamoto, T.; Yamaguchi, K. Facile Synthesis of Highly Congested 1,2-Diphosphinobenzenes from Bis(phosphine)boronium Salts. *Org. Lett.* **2006**, *8*, 6103–6106. (c) Tamura, K.; Sugiya, M.; Yoshida, K.; Yanagisawa, A.; Imamoto, T. Enantiopure 1,2-Bis(*tert*-Butylmethylphosphino)benzene as a Highly Efficient Ligand in Rhodium-Catalyzed Asymmetric Hydrogenation. *Org. Lett.* **2010**, *12*, 4400–4403. (d) Imamoto, T.; Tamura, K.; Zhang, Z.; Horiuchi, Y.; Sugiya, M.; Yoshida, K.; Yanagisawa, A.; Gridnev, I. D. Rigid P-Chiral Phosphine Ligands with *tert*-Butylmethylphosphino Groups for Rhodium-Catalyzed Asymmetric Hydrogenation of Functionalized Alkenes. *J. Am. Chem. Soc.* **2012**, *134*, 1754–1769.

(14) He, G.; Chen, S.; Wang, Q.; Huang, H.; Zhang, Q.; Zhang, D.; Zhang, R.; Zhu, H. Studies on Copper(I)-Catalyzed Highly Regio- and Stereo-Selective Hydroboration of Alkynamides. *Org. Biomol. Chem.* **2014**, *12*, 5945–5953.

(15) A more accurate description of the interaction between the *t*-Bu and Bpin groups could be possible via the NCIPLOT analysis [ref: Y. Cornaton, J.-P. Djukic, A Noncovalent Interaction Insight onto the Concerted Metallation Deprotonation Mechanism. *Phys. Chem. Chem. Phys.* **2019**, *21*, 20486–20498]. The further investigations on the exact nature of the attractive interaction between *t*-Bu and Bpin groups are underway and will be published in due course.

(16) The C-H...H-C interactions may be of minor significance for the stabilizing of these molecules. Nevertheless, we have recently reported experimental evidence showing that C-H...H-C interactions in the range of 2.3-2.7 Å are attractive and strong enough to control the equilibrium between diastereomers of a Rh-diphosphine complex [ref: I. D. Gridnev, Attraction

versus Repulsion in Rhodium-Catalyzed Asymmetric Hydrogenation. *ChemCatChem* **2016**, *8*, 3463–3465].

Table of Contents

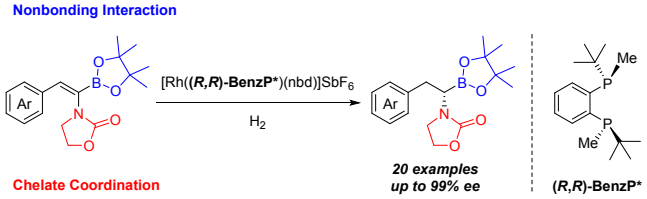

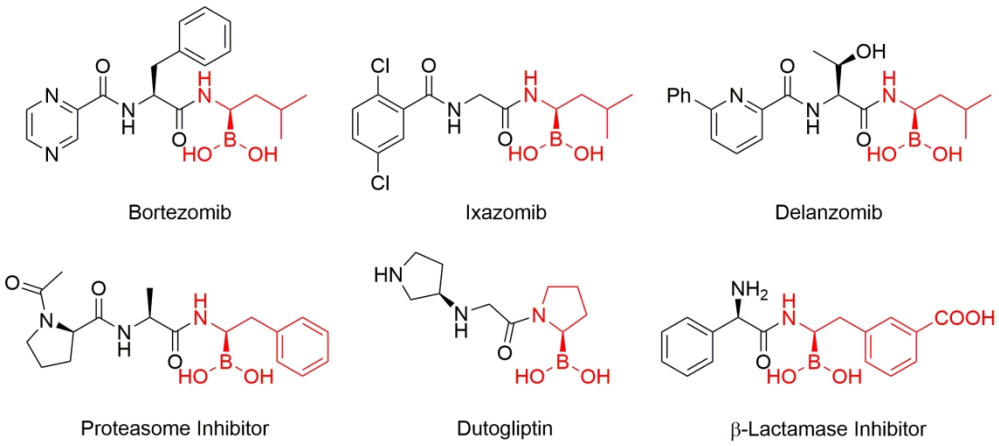

Figure 1

172x76mm (300 x 300 DPI)

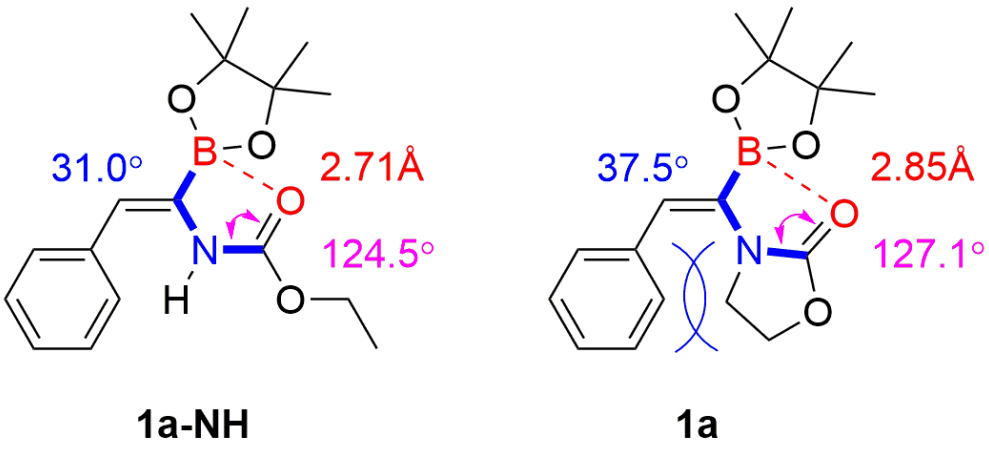

Figure 2

88x40mm (300 x 300 DPI)

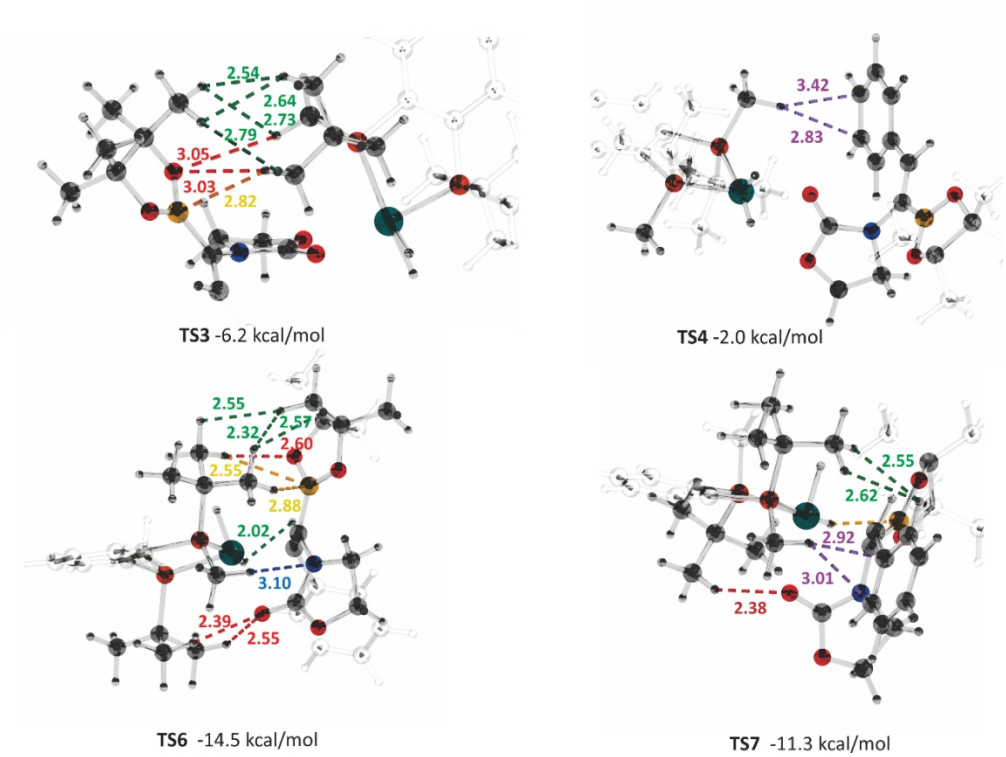

Figure 3

150x112mm (219 x 219 DPI)

a: Asymmetric borylation of imines

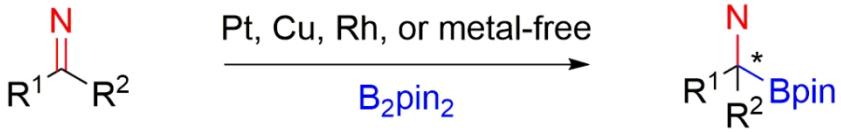

b: Asymmetric borylation of enamines

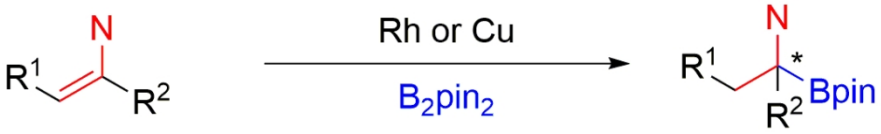

c: Asymmetric amination of alkenylboronates

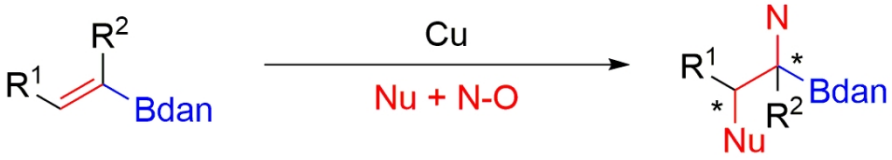

d: Asymmetric hydrogenation of α-acyl enamides

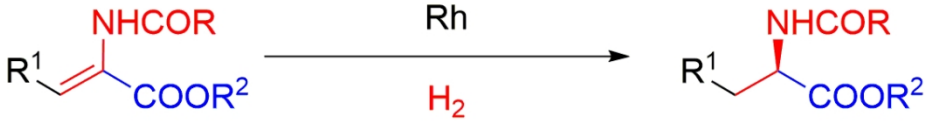

e: Asymmetric hydrogenation of α-boryl enamides

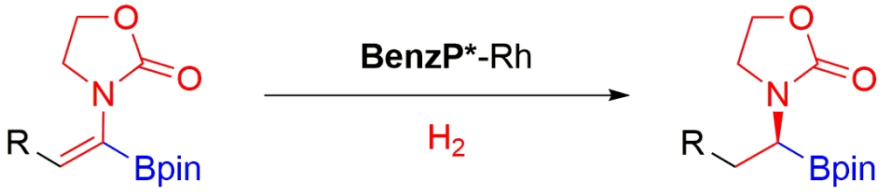

Scheme 1

98x123mm (300 x 300 DPI)

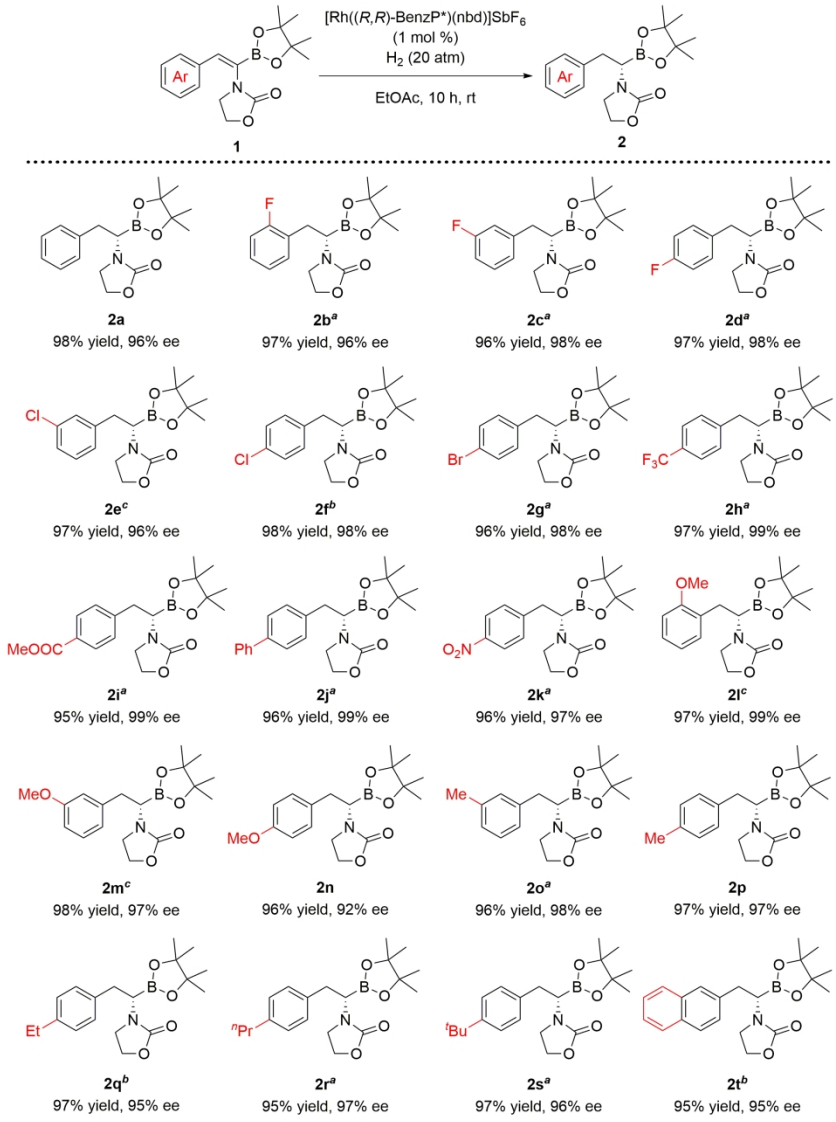

Conditions: **1** (0.1 mmol), [Rh((*R*,*R*)-BenzP*)(nbd)]SbF_6 (1 mol %), H_2 (20 atm), EtOAc (2.0 mL), rt, 10 h, unless otherwise noted. Isolated yields. The ee values were determined by HPLC using chiral columns. [a][Rh((*R*,*R*)-BenzP*)(nbd)]SbF_6 (2 mol %), 24 h. [b]24 h. [c][Rh((*R*,*R*)-BenzP*)(nbd)]SbF_6 (4 mol %), 24 h.

Scheme 2

191x276mm (300 x 300 DPI)

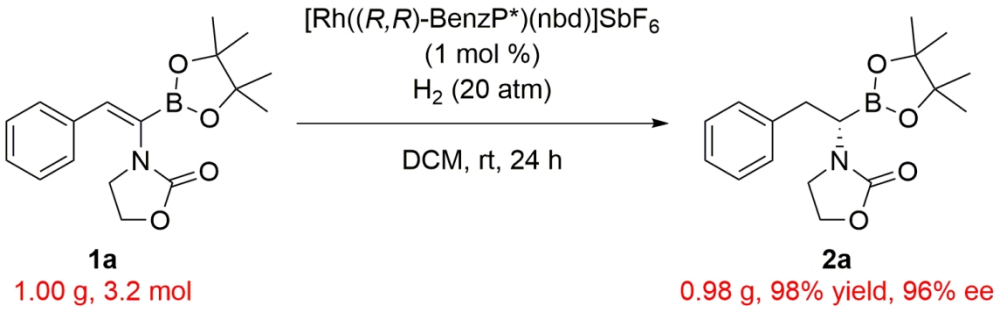

Scheme 3

130x41mm (300 x 300 DPI)

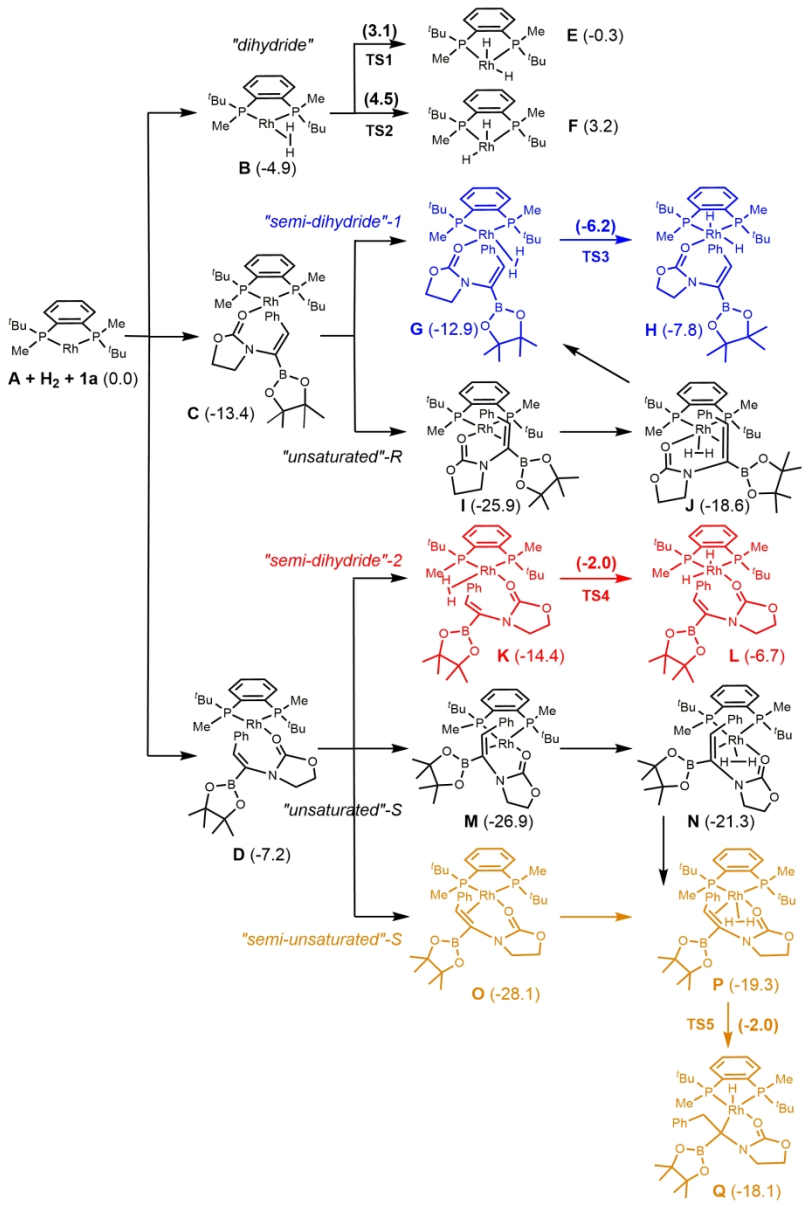

Scheme 4

165x247mm (300 x 300 DPI)

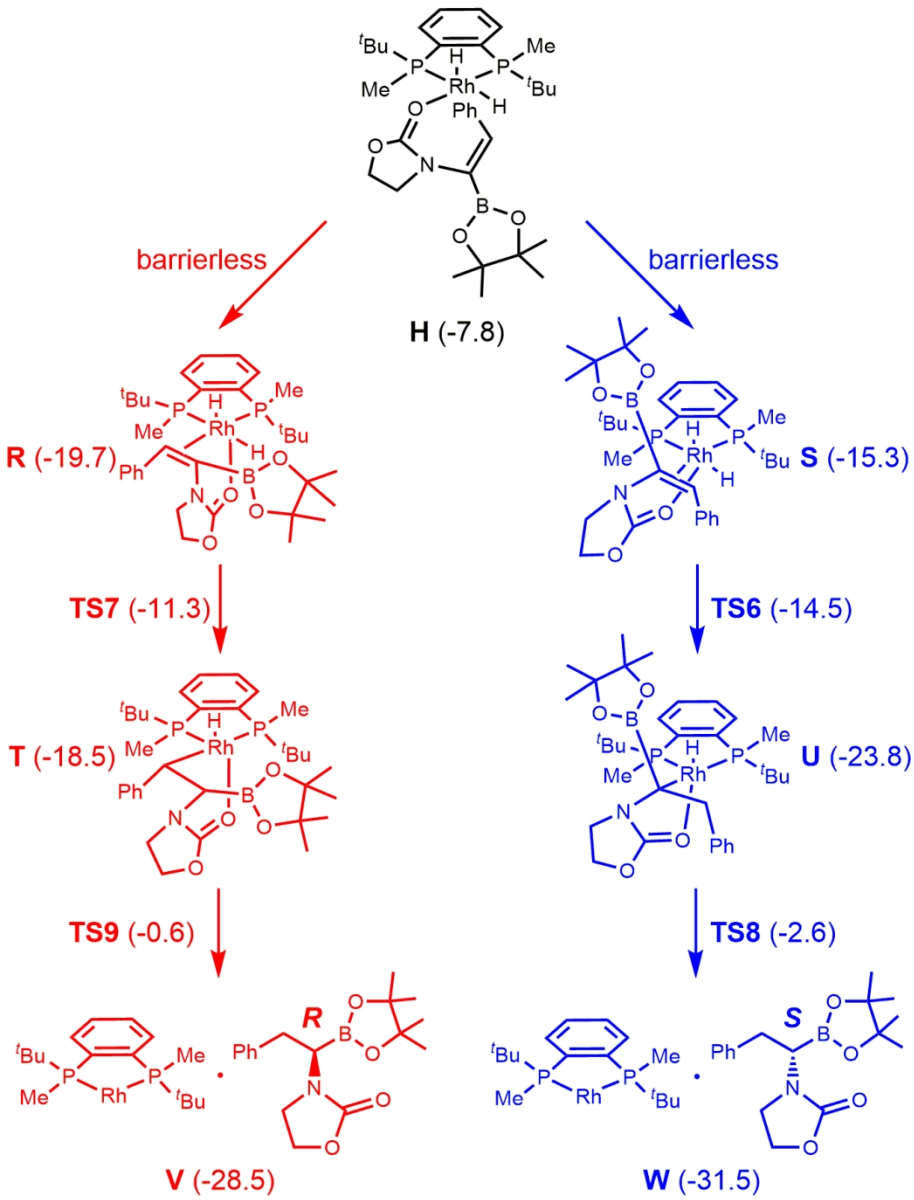

Scheme 5

115x150mm (300 x 300 DPI)

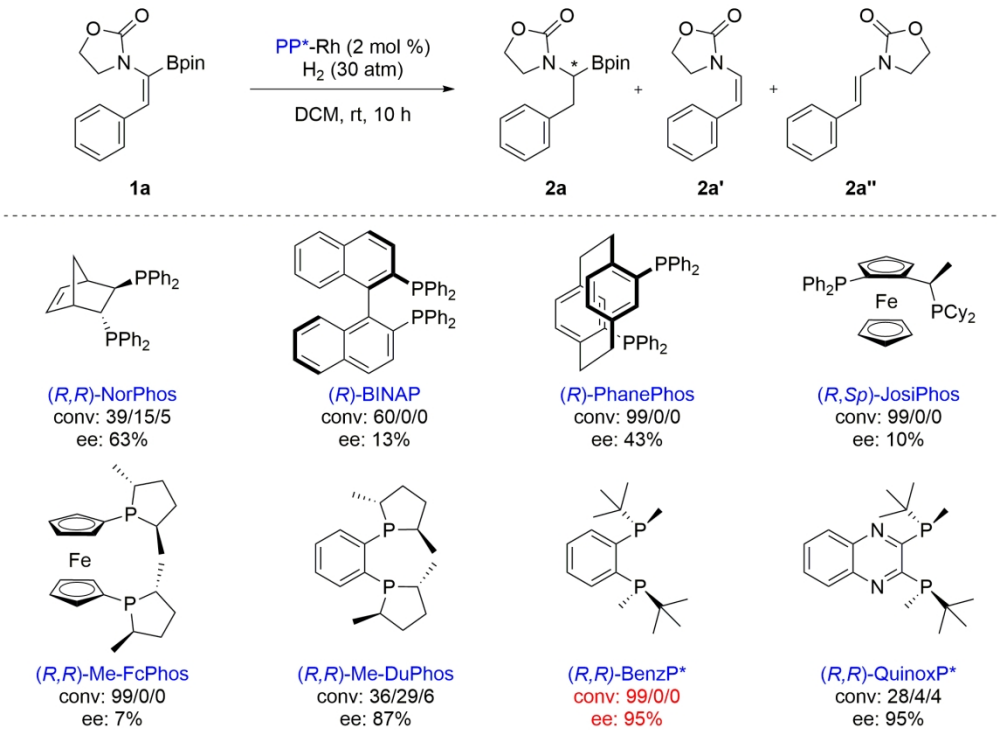

Table 1

179x131mm (300 x 300 DPI)

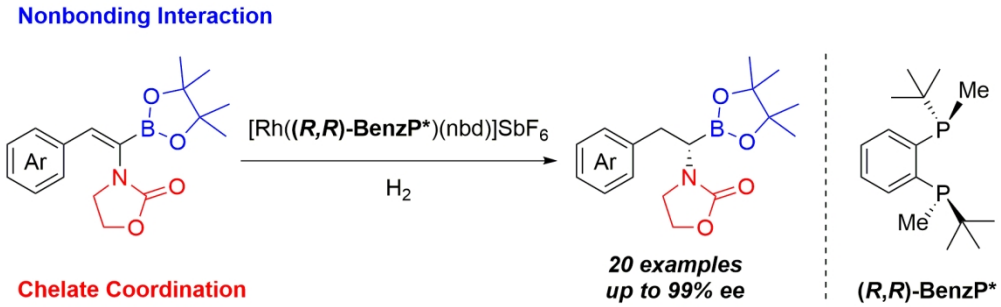

TOC

155x48mm (300 x 300 DPI)